Cardiovascular Artifact Removal for Unbiased Analysis of Intracortical EEG Signals

Dario Milea*, Vincenzo Catrambone, and Gaetano Valenza*
Neurocardiovascular Intelligence Laboratory, Bioengineering and Robotics Research Center E. Piaggio, Department of Information Engineering, School of Engineering, University of Pisa, Pisa, Italy

***Abstract*—The analysis of cortical brain recordings is significantly hindered by the presence of artifactual components, which can severely confound the interpretation of neural signals. Current methodologies, such as Independent Component Analysis (ICA), often fail to effectively reject these artifacts, particularly those originating from cardiovascular activity, without removing neurologically relevant components. This study introduces an innovative approach for the precise identification and removal of electrocardiogram (ECG)-derived artifacts from intracortical electroencephalography (iEEG) recordings. In the proposed method, the ECG signal serves as a baseline for iEEG signals, allowing the identification of cardiac artifacts. This technique ensures the retention of essential neural information, particularly during critical events, such as R-wave peaks, in brain activity analysis. The approach was evaluated using a publicly available dataset of 47 patients with simultaneous iEEG and ECG recordings suffering medication-resistant epilepsy. Experimental results reveal that our method significantly reduced the amplitude of R-peak artifacts in 85% of the recordings compared to the traditional ICA-based approach, while preserving the integrity of the underlying neural signals. Furthermore, the application of our method resulted in enhanced detection and characterization of heartbeat-evoked potentials (HEP), demonstrating its efficacy in maintaining the fidelity of brain signal interpretation. This study provides a robust tool for iEEG signals preprocessing from cardiac artifacts, allowing for an unbiased iEEG analysis, and effective iEEG-ECG brain-heart interplay studies.**

***Index Terms*—iEEG, ECG, EEG preprocessing, ICA**

I. INTRODUCTION

The study of human brain dynamics requires both high spatial and temporal resolutions, yet traditional acquisition methodologies often present substantial limitations. Human intracranial electroencephalography (iEEG) is widely recognized as the optimal solution, providing superior temporal resolution, minimal localization error, reduced susceptibility to artifacts, and an excellent signal-to-noise ratio. Due to its invasive nature, iEEG recordings are typically acquired from a very limited number of patients suffering of specific pathologic conditions, such as severe epilepsy, and iEEG recordings are needed to determine candidacy for surgical intervention [1]. Several types of intracranial electrodes have been developed for various research and clinical applications [2]. IEEG data can be collected from patients who are implanted subdurally with electrode grids (Electrocorticography, ECoG), and/or depth electrodes (stereo-electroencephalography, sEEG). ECoG utilizes grid arrays placed directly on the brain's surface, bypassing the filtering effects of the scalp and skull. Probes used in sEEG record activity from deep brain structures at precise locations within brain tissue and are used for deep-brain stimulation. Electrophysiological recordings of brain activity are often contaminated by artifacts, as any undesired signal corrupting the underlying neural dynamics [2]. Common physiological artifacts include eye movements, muscle activity, and cardiac activity, and are extensively documented in the literature [3]–[6]. These artifacts are nearly unavoidable and can severely distort recorded signals, potentially affecting the effectiveness of the analysis. Raw signals are therefore routinely preprocessed using various techniques, including filtering to remove line noise and other frequency-specific artifacts, and outliers rejection to eliminate large amplitude fluctuations caused by movement or electrode displacement. Since iEEG electrodes are placed directly within the brain, they are less susceptible to the influence of artifacts originating outside the skull, and external artifacts are generally minimized in iEEG recordings. However, the influence of ECG-related artifacts remains present. Nevertheless, cardiac activity *per se* elicits a neural response in the brain, reflecting interoceptive processing at both sensory and perceptual levels, such as the perception of heartbeats [7], and regulation of cardiac output and autonomic processes [8]. The most direct representation of brain processing of cardiac activity are the heartbeat-evoked potentials (HEP). In the most diffused EEG-based implementations, HEP are computed by averaging EEG signals time-locked to the R-peaks detected by the electrocardiogram (ECG) trace. Early studies observed HEP primarily over fronto-central regions within a $[200, 500]ms$ time window after the R-peak in the ECG signal [7]. This specific time window post R-peak, particularly localized at medial-right fronto-central sites, has been frequently interpreted as reflecting the central nervous system (CNS) representation of somatosensory information processing related to cardiac interoceptive accuracy [9]. Later components of the HEP, occurring around $[400, 600]$ms post R-peak, have been linked to various cognitive and emotional processes [8], [10]. ECG artifacts overlap with the time window of interest for HEP, impeding the identification of actual neural responses to the heartbeat, or potentially cause misleading interpretation [11]. To tackle this issue, common approaches in EEG analysis include decomposing the original

This work has received partial funding from the project Fit for Medical Robotics (Fit4MedRob) Cod. PNC0000007 (CUP B53C22006940001) and the Italian Ministry of University and Research (MIUR) in the framework of FoReLab ad CrossLab projects (Departments of Excellence).

*Corresponding Authors: dario.milea@phd.unipi.it; gaetano.valenza@unipi.it

signals through Independent Component Analysis (ICA), and subsequently identify and reject artifact-related components [12]–[14]. However, ICA can remove task-relevant signals [15]. To our knowledge, a high-performance artifact removal method specifically tailored for iEEG signals has not been proposed yet. To overcome this limitation, we propose a novel approach that exploits ECG signals as an internal reference to clean and assess intracortical brain recordings. This model was evaluated using a publicly available experimental iEEG dataset recorded during resting state.

II. MATERIALS AND METHODS

In this study, a novel technique for removing ECG artifacts from iEEG recordings has been developed and evaluated compared to a widely used approach based on ICA.

A. Experimental Dataset

The experimental dataset included iEEG and ECG signals from 47 subjects (17 females; 26 years old on average, with standard deviation of 15 years) [16]. Of the entire cohort, 31 patients were implanted with subdural ECoG grids, 5 patients underwent iEEG electrode implantation, and 11 patients were implanted with both subdural ECoG grids and iEEG electrodes. Signals were originally recorded at different sampling frequencies, i.e., $2048Hz$, $2000Hz$, or $512Hz$. All patients had medication-resistant epilepsy and underwent resting state (RS) recording, remaining silent with eyes open for up to 3 minutes. They provided signed informed consent for intracranial electrode implantation and public sharing of de-identified data for research purposes. The study was approved by the Medical Ethical Committee of the University Medical Center of Utrecht, Netherlands, in accordance with the Declaration of Helsinki (2013). The dataset is freely available at `openneuro.org/datasets/ds003688`. Further details about data acquisition can be found in [16].

B. ECG and iEEG Data Preprocessing

Signals were uniformly re-sampled at $256Hz$ for further analysis. A basic and widely used preprocessing pipeline for iEEG signals was implemented to discard generic electrical and noise artifacts [17]. This pipeline included: a $50Hz$ notch filter to remove line noise; applying a $[0.3, 70]Hz$ band pass filter; and identifying and rejecting channels based on outlier kurtosis and skewness values. ECG signals were band-pass filtered at $[0.3, 25]Hz$. R-peaks were then detected using the well-known Pan-Tompkins algorithm. To facilitate comparisons between subjects, the locations of the intracranial electrodes were transformed into the Montreal Neurological Institute (MNI) space using the FieldTrip toolbox [18]. After preprocessing, five subjects were rejected due to bad electrode location conversion, while one subject was rejected due to poor ECG channel acquisition, leading to a final total of 41 subjects' recordings.

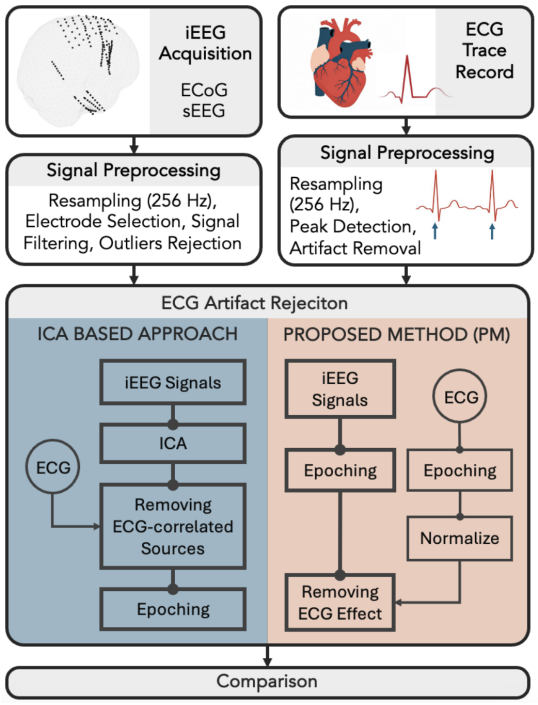

Fig. 1. **Graphical representation of the implemented analysis pipeline**

C. ICA-Based Approach:

The classic ICA-based approach decomposes the iEEG signals into independent components and identifies and rejects the ICs most correlated with ECG trace. Exemplary, for each IC, the linear Pearson's correlation coefficient (R) with the original ECG signal can be calculated. To ensure the effective representation of ECG artifacts without loss of informative content, the most correlated components are identified, and if statistically significant and having $R > 0.1$, they are rejected. Further artifactual ICs are identified and rejected as belonging to the 5% external tail of the distributions based on their standard deviation and kurtosis values. Finally, for each channel, signal epochs $S^j_{ICA}(t)$ were extracted time-locked to the R-peaks (i.e., from -200ms before the R-peak, to $+800$ms after), where the index j runs over the R-peaks.

D. Proposed Method

The influence of heart activity on the brain is proposed as a combination of the $|ECG(t)|$ trace modulated by the amplitude of the synchronous $iEEG(t)$ signal. The analysis is carried out extracting epochs time-locked to the R-peaks in the time-window $\Delta = [-200, +800]ms$ for all iEEG channels and the ECG continuous series. Thus, ECG epochs (denoted as $\Delta ECG^j(t)$) and iEEG epochs (denoted as $\Delta iEEG^j(t)$) were obtained. The segmented ECG signal is normalized within each epoch by scaling the signal to the range $[0, 1]$ as:

$$\xi^j(t) = |\Delta ECG^j(t)/max_t(|\Delta ECG^j(t)|)|. \quad (1)$$

The signal $\xi^j(t)$ serves as a mask window to suppress the QRST-complex whose electrical reverberation on the brain is

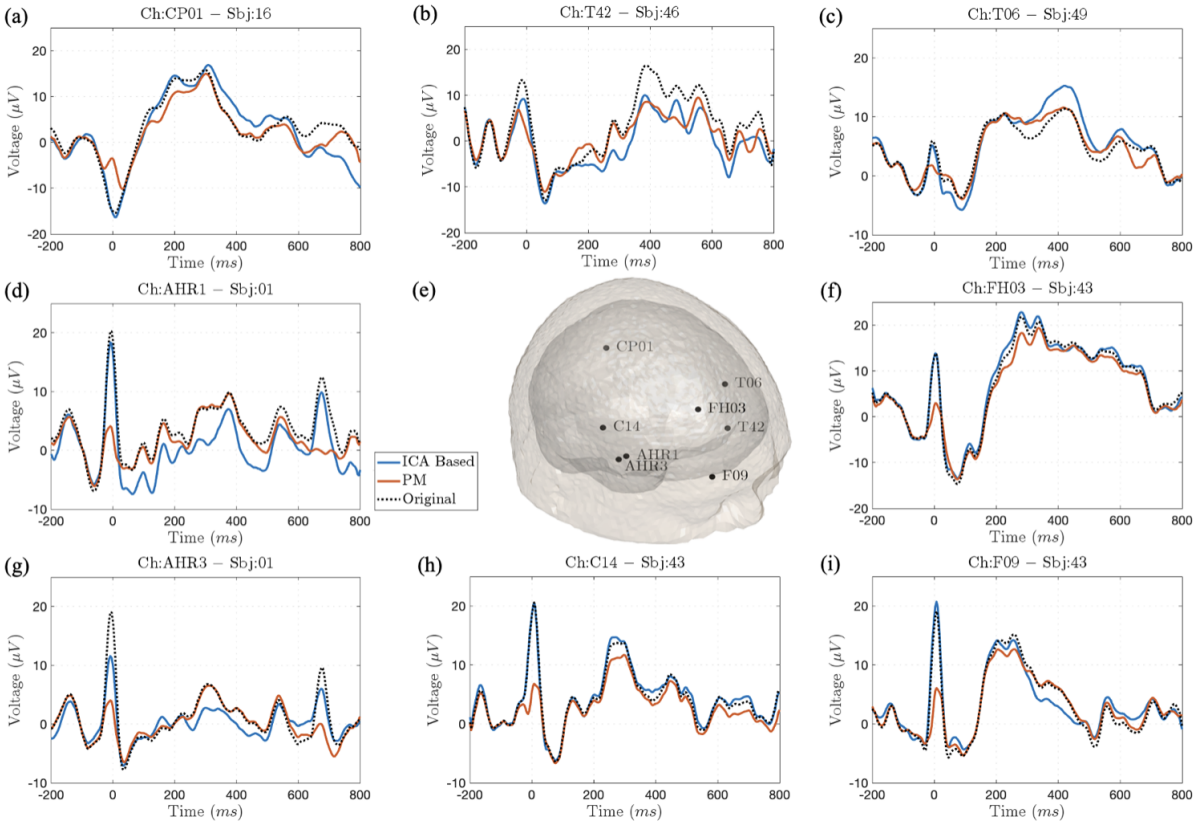

Fig. 2. **Epoch traces for distinct ECG artifact removal methods:** This Figure displays the time series of the electrode signal after processing with different methods across various electrodes. The black dotted traces represent the original average epoch without any preprocessing algorithm applied. The blue trace represents the signal after applying the ICA-based method, while the orange trace represents the signal processed using the novel proposed method (PM). Panel (a) shows channel 'CP01' from subject 16, located in the Left Occipital Medial Cortex. Panel (b) features channel 'T08' from subject 46, located in the Left Temporal Inferior Cortex. Panel (c) displays channel 'T06' from subject 49 in the Left Rolandic Operculum. Panels (d) and (g) respectively present channels 'AHR1' and 'AHR3' from subject 1, located in the Right Parahippocampal Cortex. Finally, panels (f), (h), and (i) respectively show channels 'F09', 'C14', and 'FH03' of subject 43, which are located in the Right Frontal Superior Orbital Cortex, Right Postcentral Cortex, and the Right Frontal Superior Cortex. Panel (e) illustrates the spatial location of the channels in the standardized MNI brain volume.

assumed to directly affect the iEEG signal recordings. It is used as a baseline for re-referencing each $\Delta iEEG^j(t)$ within the same time window:

$$S^j_{PM}(t) = \Delta iEEG^j(t)\big(1 - \xi^j(t)\big) \tag{2}$$

E. HEP Definition and Comparison

After ECG artifact identification and rejection algorithm, the obtained epochs (i.e., $S^j_i(t)$, where i depends on the algorithm employed, and j refers to R-peak locked epoch) were processed to identify proper heartbeat evoked potential (HEP). Firstly, outlier epochs were identified: the 1^{st} quartile $q_1(t)$, and the 3^{rd} quartile $q_3(t)$ were determined at each time sample; trials falling outside the time-varying acceptance range $\frac{1}{2}[5q_1 - 3q_3, 5q_3 - 3q_1](t)$ for more than 10% of the length were excluded from further analysis [19]. Then, each epoch underwent baseline correction by subtracting the mean value within the pre-stimulus window of $[-150, -50]ms$, and a representative mean signal epoch was estimated ($S_i(t)$) for each channel. The standard deviation (σ) for each channel was calculated within a pre-stimulus window of $[-150, -50]$ms. Finally, the signal was smoothed using a $25ms$ moving average time window. The maximum within the post-stimulus window $[150, 450]ms$ was identified, and peaks exceeding a 5σ threshold were classified as significant HEP. It must be noted that the two different ECG artifact identification and rejection algorithms lead to different series, which may or may not succeed to be classified as significant HEP. Thus meaning that the two different algorithms may lead to different number of HEP for the same subject. To further allow for a subject-wise meaningful evaluation of obtained HEP, we employed a standard brain partition into a number of region of interest (ROI) defined according to anatomical and functional criteria. Specifically, we used the automated anatomical labeling atlas (AAL), which identifies a total of 95 brain ROIs [20], and averaged across the different channels of different subjects located into each single ROI, thus obtaining ROI-specific HEP.

III. RESULTS

Figure 2 illustrates the effect of two artifact rejection methods on randomly chosen iEEG channel recordings for eight distinct channels from different subjects. This visualization

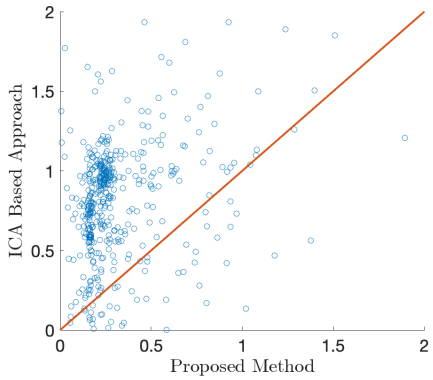

Fig. 3. The amplitude of epoch signals coincident with the R-peak is estimated for two methods and normalized relative to the amplitude of the original signal at the same time. These amplitudes are compared in a scatter plot where the x-axis refers to the PM and the y-axis represents the ICA-based approach. A red line spans the plot along the $x = y$ diagonal, indicating equal performance by both methods. Each dot represents an electrode from a subset of subjects (i.e., sbj-1, sbj-16, sbj-43, sbj-48, sbj-49).

is chosen to show the raw effect of this application without group-averaging. It is important to note that the dataset is characterized by subject-specific electrode locations due to personalized clinical requirements. The central panel (e) shows the spatial location of the analyzed electrodes with their labels, within the standardized MNI brain volume. The selected channels represent a diverse set of locations across the cortex, chosen to illustrate the range of observed responses. Each panel displays the original average epoch of the electrode (black dotted trace) and the epoch after processing with two different methods. The blue trace represents the signal after applying the ICA-based method. The orange trace represents the signal processed using the PM method. The PM method generally better attenuates the R-peak artifact compared to the ICA-based method. Furthermore, the two methods exhibit distinct effects on the post-stimulus time window, as illustrated in Figure 2, panels (c), (d), and (g). Panels (a), (f), and (i) show a case with the presence of HEP in the post-stimulus time interval $[150, 400]ms$. The positive peak, typically occurring around $300ms$ after the R-peak of the ECG, shows the brain's reaction to the heartbeat. In the other panels, the epoch traces do not show the typical evoked potential; here, the signal is flatter and noisier. To further evaluate how HEP are affected by each method, the PM and the ICA-based amplitudes were measured and normalized dividing by the corresponding amplitude of the original trace, i.e., HEP epochs derived without any specific ECG artifact preprocessing. Figure 3 presents a scatter plot of the normalized amplitudes, with the PM values plotted on the $x-$axis and the ICA-based values on the $y-$axis. Each blue dot represents a single channel from a given subject. Figure 3 reveals a denser concentration of channels along the ICA-based axis, indicating that the ICA-based values are much more distributed with respect to the PM, revealing a higher dependence of ICA-based values from the R-peak of the ECG. Across all subjects, the ICA-based approach yielded a higher amplitude peak in 85% of the data compared to the PM. The impact of the different data processing methods was also evident at the ROI level. Following the HEP identification procedure described in Section II-E, the number of identified HEP varied depending on the ECG artifact removal algorithm employed. Therefore, for each ROI, the difference in the number of HEP between the two methods was calculated and normalized by the total number of channels within that ROI. Figure 4 show the results for all the ensemble of subjects grouped by ROIs. Panel (a), reports the number of significant HEP that have been detected by the two approaches when they were at least 5 per ROI, panel (b), displays the ROIs where the normalized difference exceeded 5%. Five ROIs were identified, and the associated HEP are shown in Figure 4, panels (c-g). Orange traces represent the PM approach, while blue lines depict the ICA-based method.

IV. DISCUSSION AND CONCLUSION

This study introduces a novel technique for removing ECG artifacts from iEEG recordings, thereby mitigating their influence on the analysis of brain dynamics. This preliminary investigation focuses on resting-state data from a publicly available dataset that includes patients with ECoG and/or iEEG electrode channels, and concurrent ECG recordings. The proposed method normalizes iEEG channel traces for each epoch using the ECG trace, as illustrated in 1 and 2. Its performance was compared to an ICA-based approach involving iEEG signal decomposition and subsequent rejection of components highly correlated with the ECG signal, a common practice in EEG literature. Comparison of the two approaches revealed notable differences. PM generally demonstrated greater reliability in reducing R-peak amplitude and exhibited less dependence on ECG amplitude at the R-peaks, as shown in Figure 2, while the ICA-based approach may fail effectively removing the prominent R-peak component of the ECG artifact in several cases. Specifically, in Figure 3 PM method exhibits a denser, more concentrated channel distribution, suggesting its values are less dependent on the ECG's R-peak and potentially offer a more stable representation. The use of different data preprocessing pipelines also affects the identification of HEPs. Figure 4 shows how the number of identified HEP exceeded 5% in favor of the PM approach in 5 ROIs of the cohort it was analyzed (26 ROIs where there were at least 5 HEPs).
The performance of the proposed model may be susceptible to inter-subject variability arising from different recording settings and individual anatomical variations (e.g., skin conductivity, poor ECG signal quality), and further refinement and validation across diverse datasets and pathological conditions are needed. It is author's belief that particular attention should be paid to analyze the effects of ECG artifacts rejection algorithms on brain recordings and particularly HEP analysis. The reported results are promising and normalizing the ECG trace for each epoch seems to help mitigate the artifacts propagation. We conclude that the proposed approach represents a promising tool for leveraging the fundamental information carried by iEEG recordings.

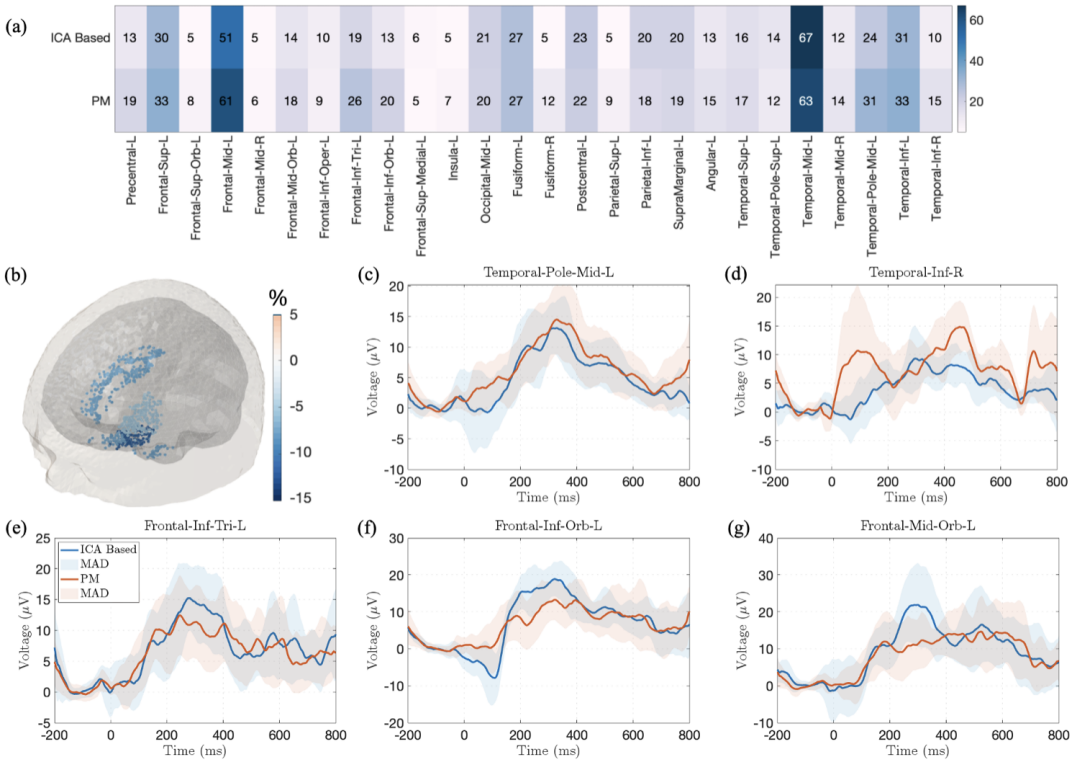

Fig. 4. Panel (a) show the number of HEP that have been detected by the two approaches when they were at least 5 per ROI. Panel (b) depicts the difference in the number of HEP between the two methods, normalized by the total number of channels within each ROI. Only the ROIs where the relative difference exceeds 5% are shown. Panels (c-g) display the median trace for each ROI and the median absolute deviation (MAD) as shaded area. PM traces are depicted in orange, while ICA-based ones in blue.

REFERENCES

[1] B. C. Jobst *et al.*, "Intracranial eeg in the 21st century," *Epilepsy currents*, vol. 20, no. 4, pp. 180–188, 2020.

[2] M. R. Mercier *et al.*, "Advances in human intracranial electroencephalography research, guidelines and good practices," *Neuroimage*, vol. 260, p. 119438, 2022.

[3] M. Kern *et al.*, "Heart cycle-related effects on event-related potentials, spectral power changes, and connectivity patterns in the human ecog," *Neuroimage*, vol. 81, pp. 178–190, 2013.

[4] M. Kern *et al.*, "Blink-and saccade-related suppression effects in early visual areas of the human brain: Intracranial eeg investigations during natural viewing conditions," *NeuroImage*, vol. 230, p. 117788, 2021.

[5] T. Ball *et al.*, "Signal quality of simultaneously recorded invasive and non-invasive eeg," *Neuroimage*, vol. 46, no. 3, pp. 708–716, 2009.

[6] K. Jerbi *et al.*, "Saccade related gamma-band activity in intracerebral eeg: dissociating neural from ocular muscle activity," *Brain topography*, vol. 22, no. 1, pp. 18–23, 2009.

[7] O. Pollatos *et al.*, "Accuracy of heartbeat perception is reflected in the amplitude of the heartbeat-evoked brain potential," *Psychophysiology*, vol. 41, no. 3, pp. 476–482, 2004.

[8] M. A. Gray *et al.*, "A cortical potential reflecting cardiac function," *Proceedings of the National Academy of Sciences*, vol. 104, no. 16, pp. 6818–6823, 2007.

[9] M.-P. Coll *et al.*, "Systematic review and meta-analysis of the relationship between the heartbeat-evoked potential and interoception," *Neuroscience & Biobehavioral Reviews*, vol. 122, pp. 190–200, 2021.

[10] M. Baranauskas *et al.*, "Brain responses and self-reported indices of interoception: Heartbeat evoked potentials are inversely associated with worrying about body sensations," *Physiology & behavior*, vol. 180, pp. 1–7, 2017.

[11] W. Lee *et al.*, "Heartbeat-related spectral perturbation of electroencephalogram reflects dynamic interoceptive attention states in the trial-by-trial classification analysis," *NeuroImage*, vol. 299, p. 120797, 2024.

[12] M. Ullsperger *et al.*, *Simultaneous EEG and fMRI: recording, analysis, and application*. Oxford University Press, 2010.

[13] F. C. Viola *et al.*, "Using ica for the analysis of multi-channel eeg data," *Simultaneous EEG and fMRI: Recording, Analysis, and Application: Recording, Analysis, and Application*, pp. 121–133, 2010.

[14] S. Hoffmann *et al.*, "The correction of eye blink artefacts in the eeg: a comparison of two prominent methods," *PloS one*, vol. 3, no. 8, p. e3004, 2008.

[15] F. H. Petzschner *et al.*, "Focus of attention modulates the heartbeat evoked potential," *NeuroImage*, vol. 186, pp. 595–606, 2019.

[16] J. Berezutskaya *et al.*, "Open multimodal ieeg-fmri dataset from naturalistic stimulation with a short audiovisual film," *Scientific Data*, vol. 9, no. 1, p. 91, 2022.

[17] L. J. Gabard-Durnam *et al.*, "The harvard automated processing pipeline for electroencephalography (happe): standardized processing software for developmental and high-artifact data," *Frontiers in neuroscience*, vol. 12, p. 97, 2018.

[18] R. Oostenveld *et al.*, "Fieldtrip: open source software for advanced analysis of meg, eeg, and invasive electrophysiological data," *Computational intelligence and neuroscience*, vol. 2011, no. 1, p. 156869, 2011.

[19] L. Citi *et al.*, "Documenting, modelling and exploiting p300 amplitude changes due to variable target delays in donchin's speller," *Journal of Neural Engineering*, vol. 7, no. 5, p. 056006, 2010.

[20] N. Tzourio-Mazoyer *et al.*, "Automated anatomical labeling of activations in spm using a macroscopic anatomical parcellation of the mni mri single-subject brain," *Neuroimage*, vol. 15, no. 1, pp. 273–289, 2002.